EPSC Abstracts
Vol. 11, EPSC2017-480, 2017
European Planetary Science Congress 2017

Mini-RF bistatic observations of Copernican crater ejecta on the Moon

A.M. Stickle, G.W. Patterson, J.T.S Cahill, and the Mini-RF Team
Johns Hopkins Applied Physics Laboratory, 11100 Johns Hopkins Rd., Laurel, MD, USA 20723, (angela.stickle@jhuapl.edu/ Fax: +1-240-228-8939)

Abstract

The Mini-RF radar is current operating in a bistatic configuration using the Goldstone DSS-13 and Arecibo Observatory as transmitters in X-band (4.2-cm) and S-band (12.6 cm), respectively. A typical product examining the scattering properties of the lunar surface that can be derived from backscattered microwave radiation is the Circular Polarization Ratio (CPR). Here, we examine the ejecta blankets of Copernican aged craters on the lunar surface in both S- and X-band to examine the scattering properties of young crater ejecta. Several observed craters exhibit a clear opposition effect at low bistatic (phase) angles. This opposition effect is consistent with optical studies of lunar soils done in the laboratory, but these observations are the first time this effect has been measured on the Moon at radar wavelengths. Differences in the CPR behaviour as a function of bistatic angle may also provide opportunities for relative age dating between Copernican craters.

1. Introduction

The Mini-RF instrument aboard NASA's Lunar Reconnaissance Orbiter (LRO) is currently acquiring bistatic radar data of the lunar surface at both S-band (12.6 cm) and X-band (4.2 cm) wavelengths in an effort to understand the scattering properties of lunar terrains as a function of phase angle. Previous work, at optical wavelengths, has demonstrated that the material properties of lunar regolith can be sensitive to variations in phase angle [1-3]. This sensitivity gives rise to the lunar opposition effect and likely involves contributions from shadow hiding at low phase angles and coherent backscatter near zero phase [1]. Mini-RF bistatic data of lunar materials indicate that such behavior can also be observed for lunar materials at the wavelength scale of an S-band radar (12.6 cm). The ejecta blankets of seven lunar craters have been observed to date, and the Circular Polarization Ratio (CPR) examined as a function of

1.1 Bistatic Observation Campaign

Radar observations of planetary surfaces provide important information on the structure (i.e., roughness) and dielectric properties of surface and buried materials [4-7]. These data can be acquired using a monostatic architecture, where a single antenna serves as the signal transmitter and receiver, or they can be acquired using a bistatic architecture, where a signal is transmitted from one location and received at another. The former provides information on the scattering properties of a target surface at zero phase. The latter provides the same information but over a variety of phase angles. NASA's Mini-RF instrument on the Lunar Reconnaissance Orbiter is currently operating in a bistatic architecture with the Arecibo Observatory in Puerto Rico and the Goldstone DSS-13 antenna in California. The Arecibo Observatory serves as the transmitter for S-band operations and DSS-13 serves as the transmitter for X-band operations. In both cases and Mini-RF serves as the receiver. This architecture maintains the hybrid dual-polarimetric nature of the Mini-RF instrument [8] and, therefore, allows for the calculation of the Stokes parameters (S_1, S_2, S_3, S_4) that characterize the backscattered signal (and the products derived from those parameters).

2. Observations

A common product derived from the Stokes parameters is the Circular Polarization Ratio (CPR),

$$\mu_C = \frac{(S_1 - S_4)}{(S_1 + S_4)} \quad (1).$$

CPR information is commonly used in analyses of planetary radar data [4-7], and is a representation of surface roughness at the wavelength scale of the radar (i.e., surfaces that are smoother at the wavelength scale will have lower CPR values and surfaces that are rougher will have higher CPR

values). High CPR values can also serve as an indicator of the presence of water ice [9].

As part of the Mini-RF bistatic observation campaign, CPR information for a variety lunar terrains is being collected over a range of bistatic and incidence angles. The first campaign (during LRO extended mission targeted a variety of Copernican-aged impact craters in order to characterize the opposition response of materials known to be rough at radar wavelengths [10]. Patterson et al. [10] showed the ejecta properties for three of these craters: Byrgius A, Kepler, and Bouguer, as a function of bistatic angle. Both Kepler and Bygius A exhibited an opposition effect, while Bouguer did not. The opposition responses of Byrgius A and Kepler ejecta lead to increases in CPR of ~30% and 15%, respectively, as bistatic angle approaches 0°. The mean CPR of Byrgius A and Kepler ejecta at bistatic angles outside of their opposition responses averages ~20% higher than surrounding materials. The mean CPR of Bouguer averages ~5% above surrounding materials. Patterson et al. [10] suggest that the radar scattering characteristics of the continuous ejecta for these three craters, coupled with age estimates based on crater statistics and geologic mapping, suggest a relationship between the opposition response of the ejecta and the age of the crater (i.e., Byrgius A is the youngest of the craters observed and shows the strongest response). Thus, describing the CPR response as a function of phase angle may be a way to determine relative age between deposits. Here, we examine the ejecta of eight Copernican aged craters and document CPR characteristics as a function bistatic angle in order to test that hypothesis. The spatial resolution of the data varied from one observation to another, as a function of the viewing geometry, but averaged ~100 m.

Four of the examined craters exhibit CPR characteristics suggestive of an opposition effect in S-band: higher CPR at lower bistatic (phase) angle (Figure 1). X-band observations of Anaxagoras also suggest an opposition surge at low bistatic angle, though relatively constant CPR in S-band at higher bistatic angles. The increase in CPR occurs near 2-4 degrees bistatic angle. These craters occur in both highlands and mare regions, and are all characterized as young. Three other examined craters exhibit CPR that remains relatively constant across phase angle. This may be for a couple reasons. 1) The craters are older (though still Copernican), and so the opposition effect will be less pronounced, or 2) there are few observations of these craters, with none to few over very small angles. An opposition effect may be present, and not yet observed. Both Schomberger A and Kepler exhibit unique scattering properties as a function of bistatic angles, with areas of relatively constant CPR at various CPR values. Continuing observations are targeting these regions to increase the phase angle coverage. Additional study is ongoing to fully characterize the CPR response with viewing geometry for these young craters. All of these targets will also be targeted in X-band, as well as adding additional craters (e.g., Schomberger, Copernicus).

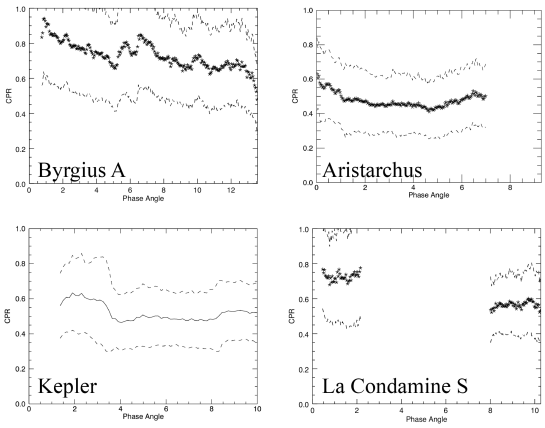

Figure 1. CPR as a function of phase for 4 examined craters. All four craters here exhibit differences in CPR with bistatic angle, with higher CPR at lower bistatic angles (characteristic of an opposition effect).

Acknowledgements

This work was funded by the NASA LRO and Mini-RF projects.

References

[1] Hapke et al. (1998), *Icarus*, 133, 89-97; [2] Nelson et al. (2000), *Icarus*, 147, 545-558; [3] Piatek et al. (2004), *Icarus*, 171, 531-545. [4] Campbell et al. (2010), *Icarus*, 208, 565-573; [5] Raney et al. (2012), *JGR,* 117, E00H21; [6] Carter et al. (2012), *JGR,* 117, E00H09; [7] Campbell (2012), *JGR*, 117, E06008; [8] Raney, R. K. et al. (2011), *Proc. of the IEEE*, 99, 808-823; [9] Black et al. (2001), *Icarus*, 151, 167-180;[10] Patterson, et al. (2017), *Icarus*, 283, 2-19; [11] Morota et al. (2009) *Met. Planet. Sci.* 44(8), 1115-1120; [12] Koenig et al. (1977) *Proc. LPSC*, 8, p. 555; [13] Baldwin (1985) *Icarus* 61, 63-91; [14] Ulrich (1969) USGS Map I-604(LAC-11)